

## The relationships between *Brucella melitensis* predilection sites, bacterial loads in vivo, and the agglutinating antibody response in experimentally infected sheep

Xiaolei GAO, Yu KUANG, Lintao MA, Yanli LU, Qingmin WU\*

Key Laboratory of Animal Epidemiology and Zoonosis of the Ministry of Agriculture, College of Veterinary Medicine, China Agricultural University, Beijing, P.R. China

Received: 31.10.2014

Accepted/Published Online: 13.02.2015

Printed: 10.06.2015

**Abstract:** For exploring *Brucella melitensis* survival in in vivo predilection sites and the relationship between bacterial loads and the detection of antibody titers in experimentally subcutaneously infected sheep with *B. melitensis* 16M, ten rams and ten ewes were used. One ram and one ewe were euthanized at 7, 15, 30, 60, 90, 120, and 180 days post inoculation (dpi). Bacteriological results showed that tissue isolation rates and bacterial loads peaked from 7 dpi to 30 dpi and then cleared until 120 dpi. In in situ hybridization trials the strongest signals for *B. melitensis* were detected at 7 dpi and 15 dpi, and then they gradually cleared. Monitoring results of agglutinating antibodies showed that anti-*Brucella* antibodies began to be produced at 7 dpi, peaked at 15 dpi, and gradually declined until lower detection levels than the threshold were being detected at 180 dpi. Thus, we found that the more *Brucella* bacterial loads there were in vivo, the higher the antibody titers were in sera, which suggested that detection of the agglutinating antibody titers might be used as an indicator of a *Brucella* carrier in infected animals.

**Key words:** *Brucella melitensis*, bacterial loads, in situ hybridization, antibody response

### 1. Introduction

Brucellosis is a global zoonosis, induced by *Brucella* spp., that is characterized by abortion, weak birth of offsprings in pregnant females, and infertility in females and males (1,2). It is known that *Brucella abortus* is an infection maintained through life and distributed in the uterus to the fetus and placenta, and to the lymph nodes and other organs and tissues in calves (3). Sheep and goats were both used as host models to study the pathogenesis, tissue distributions, and persistence in experimental infection of *B. abortus* and *B. melitensis*. Suraud et al. reported that the early distribution of *B. melitensis* in experimentally infected sheep is a local and systemic dissemination, mainly in the tonsils, local and peripheral lymph nodes, and spleen (4). Duran-Ferrer et al. reported the changes in pathology, immunology, and bacterial loads in experimentally nonvaccinated pregnant ewes (5). However, little is known about the serological and bacteriological variation features of the different infection phases in animals infected by *Brucella* spp.

Brucellosis can be transmitted to humans by nonpasteurized milk and other products of cows, sheep, and goats (6,7) or by direct contact with infected animals or carcasses (8). The clinical manifestations and

histopathological changes in the infected animals depend on animal species, breed, age, immunological status, sexual maturity, and pregnancy stage of the animal and the inoculation route, dose, and virulence of *Brucella* (9). In the prevention and control of brucellosis in both humans and animals, *Brucella* carrier animals are important targets, and animals with positive antibodies against brucellosis have traditionally been culled out. *Brucella* carrier animals, and especially the ones overloaded by *Brucella* spp., should definitely be culled and destroyed in the animal brucellosis eradication campaign, while *Brucella*-free animals might be important seed selection for antibrucellosis animal breeding, although they might have weak serological positive reactions. Therefore, it is important to explore methods for indicating bacterial loads in vivo in infected animals.

In this study, ten rams and ten nonpregnant ewes were selected and subcutaneously inoculated with *B. melitensis* 16M for exploration of the relationships between bacterial loads and antibody titers in the experimental infected animals. The results might provide the basis for preventing excessive culling of animals and resource waste in animal brucellosis eradication campaigns.

\* Correspondence: wuqm@cau.edu.cn

## 2. Materials and methods

### 2.1. Bacteria and bacterial culturing

The *B. melitensis* 16M (CVCC 7002) used was originally from the China Veterinary Culture Center; it is a smooth phenotype virulent strain. This strain was routinely cultured on tryptic soy agar (TSA, Bacto) or tryptic soy broth at 37 °C. The colony-forming units (CFUs) of the bacterial inoculum were determined before and after infection. All work with live virulent *Brucella* strains was performed in biosafety level 3 facilities at the China Agricultural University.

### 2.2. Animals and the experimental infection

To determine the tissue distribution of *Brucella* in infected animals, 10 rams and 10 nonpregnant ewes of 10 months of age were obtained from brucellosis-free regions and determined to be seronegative with the brucellosis Rose-Bengal plate agglutination test (10) and a standard tube agglutination test (11). *B. melitensis* 16M was subcutaneously inoculated at a dose of  $1 \times 10^9$  CFU per animal. After infection, the animals were housed in restricted large-animal isolation facilities. Another group of four sheep (two rams and two ewes) was maintained in conventional housing as the uninfected control group. The infected sheep were examined daily for evidence of disease. At 7, 15, 30, 60, 90, 120, and 180 days post infection (dpi), one ewe and one ram were euthanized by electric shock to enable gross observation and tissue sampling. At 360 dpi, all the remaining animals were euthanized for bacterial isolation and antibody tests. The bodies were disposed of according to relevant national regulations. All experiments involving animals followed the regulations enacted by the Beijing Administration Office of Laboratory Animals.

### 2.3. Serological examination

To evaluate the antibody response, 2 mL of blood was collected from the jugular vein of each inoculated sheep before infection and at 7, 15, 30, 60, 90, 120, 180, 240, and 360 dpi. Sera were stored at -20 °C in aliquots until tested. The *Brucella*-specific antibody in sera was determined by microagglutination test (MAT) with a commercial *Brucella* antigen (purchased from the China Institute of Veterinary Drug Control) according to accepted procedures (10,11).

### 2.4. Tissue sampling

After the sheep were euthanized, a total of 23 samples were collected from each sheep, which included the liver, spleen, lungs, heart, kidneys, skeletal and smooth muscles, duodenum, jejunum, ileum, abomasum, bladder, lymph nodes (parotid, submaxillary, inguinal, iliac, prescapular, mesenteric, portal, hilar, and reniportal lymph nodes), mammary glands/testes, and uterine horn/epididymis. All the samples were cut into two pieces; one piece was fixed in 10% neutral buffered formalin for in situ hybridization (ISH) (12) and the other was used for bacteriological examination.

### 2.5. Bacteriological examination

Before bacteriological examination, all the samples (except the duodenum, jejunum, ileum, abomasum, and bladder) were aseptically trimmed and weighed, then homogenized in 1 mL of sterile phosphate buffered saline, serially diluted, and plated onto TSA with 200 µL of homogenates of each sample. The bacterial number was determined by 3–5 days of incubation at 37 °C in 5% CO<sub>2</sub> and expressed as log<sub>10</sub> per gram (13).

### 2.6. Preparation of DNA probe and its evaluation

For detecting the *B. melitensis* DNA, a probe was prepared from the genomic DNA of *B. melitensis* 16M by PCR using the following primers (14): IS711-specific primer F 5'- TGC CGA TCA CTT AAG GGC CTT CAT -3' and *B. melitensis*-specific primer R 5'- AAA TCG CGT CCT TGC TCG TCT GA -3'. Briefly, after the PCR product was amplified, the sequencing was done and compared to the NCBI database. The PCR product was then cloned into the *pEAZY-T1* Simple Cloning Vector (Beijing TransGen Ltd.), which was transformed into the *Trans1-T1* Phage Resistant Chemically Competent Cell (Beijing TransGen Ltd.). The recombinant plasmid was isolated and confirmed by PCR using the primers used in the experiment. The purified plasmid was used to synthesize and label DNA probes according to the instructions of the kit. The probe was labeled by digoxigenin (DIG)-dUTP (DIG-Nick Translation Mix, Roche). One microgram of recombinant plasmid was added to sterile double-distilled water with a final volume of 16 µL, 4 µL of DIG-Nick Translation Mix was added, and this mixture was centrifuged briefly. The mixture was incubated for 90 min at 15 °C and then the reaction was placed on ice. Three microliters from a 20-µL reaction volume was pipetted out for examination of the size of the probe on an agarose minigel. When the synthesized probe ranged between 200 and 500 bp in length, the reaction was stopped by heating to 65 °C for 10 min. Finally, the probe was separated into aliquots and stored at -20 °C until use. The sensitivity of synthesized probe was detected as per the instructions of the DIG Luminescent Detection Kit (Roche). Briefly, the synthesized probe was diluted at 1:10, 1:100, 1:1000, 1:10,000, and 1:100,000. The diluted probes and DIG-labeled control DNA in the kit were loaded onto a nitrocellulose membrane. The spotting membrane was heated to 120 °C for 10 min, rinsed in washing buffer, incubated in 10 mL of blocking solution for 30 min at room temperature, incubated for 30 min at 37 °C in 10 mL of antibody solution, washed with 10 mL of washing buffer for 2 × 15 min, and equilibrated in 20 mL of detection buffer for 5 min. The spotting membrane was immersed in 1 mL of diluted CSPD solution according to the protocol of the kit for 5 min at room temperature, and then the liquid was drained and the membrane was incubated for 10 min at 37 °C again. Finally, the spotting

membrane was exposed to X-ray film for 15 min at room temperature. The optimal dilution was used in the following ISH examinations.

### 2.7. In situ hybridization procedures

For ISH examination, all the tissue samples collected were fixed in 10% neutral buffered formalin, and sections of 5  $\mu\text{m}$  in thickness of each sample were used for ISH analysis. Prior to hybridization, the sample sections were completely fused to the slides, and then the paraffin was removed and they were prepared for rehydration. The slides were washed with xylene two times each for 5 min, two times each for 5 min with 100% ethanol, again with 95% ethanol for 5 min and with 70% ethanol for 5 min, and then with distilled water for 5 min. After that, the sample sections were permeabilized in 0.1 N HCl for 30 min, rinsed in distilled water, acetylated in triethanolamine (TEA)-hydrochloride (HCl) buffer (0.5 M TEA-HCl, 0.75 M NaCl, pH 8.0) with 0.25% acetic anhydride for 10 min, and rinsed in distilled water. Finally, the sample sections were dehydrated in 70% ethanol for 5 min and allowed to air-dry (12). To decrease the background, the slides were allowed to prehybridize at 55  $^{\circ}\text{C}$  for 1 h with hybridization buffer containing 50% deionized formamide, 10% dextran sulfate, 0.1% sodium pyrophosphate, 0.05% sodium dodecyl sulfonate, 2X SSC (0.3 M sodium chloride, 0.03 M sodium citrate, pH 7.0), 5X Denhardt's solution, and 1 mg/mL denatured salmon sperm DNA (Sigma). Each of 10 sections was hybridized in 0.5 mL of hybridization mixture consisting of 50% deionized formamide, 10% blocking reagent, 10% dextran sulfate, 5X Denhardt's solution, 4X SSC, 10 mg/mL denatured salmon sperm, and 5  $\mu\text{g}/\mu\text{L}$  DIG-labeled DNA probe at 60  $^{\circ}\text{C}$  for 18–20 h in a humid box to prevent drying out.

After hybridization, the slides were washed to remove the unbound portions. Posthybridization washes were performed on a stirring plate with 4X SSC/50% formamide two times each for 30 min (at 60  $^{\circ}\text{C}$ ), 2X SSC/50% formamide two times for 20 min (at 50  $^{\circ}\text{C}$ ), 1X SSC/50% formamide two times for 15 min (at 42  $^{\circ}\text{C}$ ), and 0.5X SSC for 20 min (at 37  $^{\circ}\text{C}$ ), then rinsed in distilled water at room temperature. Subsequently, the bound probe was detected with 1:500 alkaline phosphatase-conjugated anti-DIG antibody and developed into color in BCIP/NBT solution by applying the DIG Detection Kit (Roche). Finally, the sections were counterstained with nuclear fast red and mounted under coverslips (12). Tissues from the noninfected sheep were used as a negative control. In addition, negative controls were included in the replacement of the DIG-labeled DNA probe of hybridization buffer.

## 3. Results

### 3.1. Clinical and gross pathological changes observation

All infected sheep developed transient (48 h) low fever and anorexia after infection. To gain insights into the pathological changes associated with the infection, autopsies were performed at various time points. At 7 and 15 dpi, mild swelling was observed in the submandibular and prescapular lymph nodes. At 30 dpi, the liver, spleen, and prescapular lymph nodes were generally mildly enlarged, but distinct changes were not observed on the cutting surfaces. After 60 dpi, no obvious lesions were observed in any organs or tissues.

### 3.2. Dynamics of the specific *Brucella* agglutinating antibodies

All experimentally infected sheep were seronegative for brucellosis before infection. However, specific anti-*Brucella* antibodies developed after infection. The evolution of the serological response after infection by MAT test is shown in Figure 1.

All sheep produced the specific antibodies at 7 dpi and peaked at 15 dpi. The antibody titers then progressively declined until the antibody detection threshold was reached at 180 dpi and the agglutination phenomenon did not appear from 240 to 360 dpi.

### 3.3. Spatial and temporal distributions of *B. melitensis* 16M in infected sheep

For routine bacteriological examination, 36 samples from each infected sheep were collected at different times postinfection for *Brucella* detection, and the results were as follows: 50.0% (18/36) at 7 dpi, 68.42% (26/36) at 15 dpi, 55.56% (20/36) at 30 dpi, 52.78% (19/36) at 60 dpi, 22.22% (8/36) at 90 dpi, and 2.03% (1/36) at 120 dpi for *Brucella* detection. The positive rate of tested samples was highest at 15 dpi, and then it declined gradually.

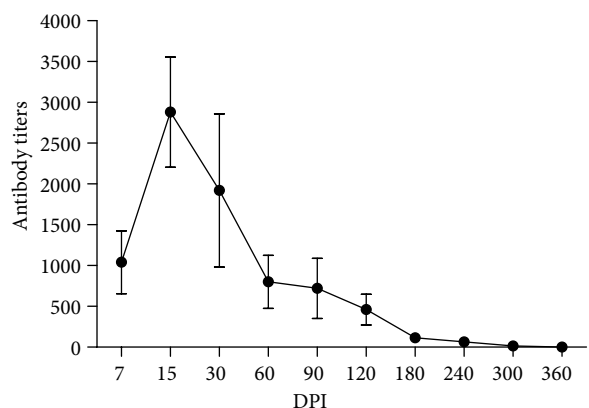


**Figure 1.** Serum antibody responses of sheep inoculated subcutaneously with *B. melitensis* 16M as measured by MAT using *B. melitensis* antigen. The serum antibody was detected in duplicate, and error bars indicate SD.

The evolution of the degree of infection, expressed as the mean CFUs isolated in samples, is shown in Figure 2; organs bacteriologically confirmed as negative are not listed. In general, the *B. melitensis* strain was detected in most of the organs and tissues at 15 dpi, and it persisted for 3 months in some samples. Among the infected sheep, the spleen and most superficial lymph nodes (prescapular, parotid, and submaxillary lymph nodes) were the main target organs, in which large numbers of *Brucella* were isolated at 15 dpi. The bacteria were then gradually cleared, and no bacteria were isolated from any samples after 120 dpi. In the other organs such as the heart, liver, lungs, kidneys, cerebrum, testes, and epididymis, the bacteria were short-lived after infection and then gradually cleared in vivo. In addition, no *B. melitensis* was isolated from skeletal elements, smooth muscle, bladder, or uterine horn throughout the period of experiment in the routine bacteriological examination.

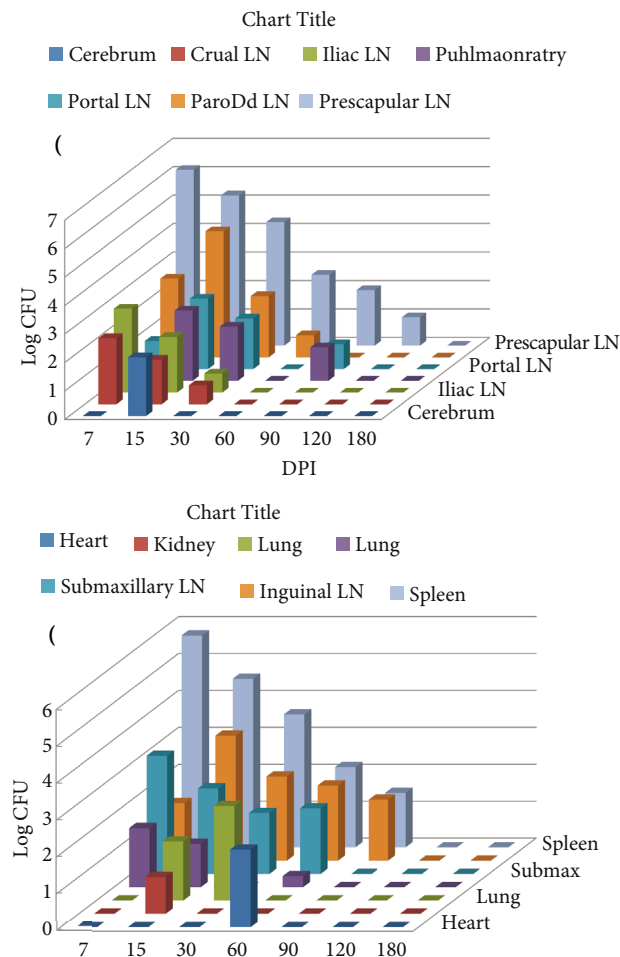


**Figure 2.** Kinetics of infection and evolution of infected tissues infected by *B. melitensis* 16M after subcutaneous vaccination in sheep (A, B). The number of live *B. melitensis* 16M expressed as log<sub>10</sub> CFU per gram. The results in some tissues are not present, since they were always bacteriologically negative.

### 3.4. ISH detection

In ISH examination, the detection rates for test samples were as follows: 78.26% (36/46) at 7 dpi, 82.61% (38/46) at 15 dpi, 69.57% (32/46) at 30 dpi, 39.13% (18/46) at 60 dpi, 10.87% (5/46) at 90 dpi, and 2.17% (1/46) at 120 dpi for DNA signals in the examined sections. The positivity rate of test samples was highest at 15 dpi; it declined progressively and cleared after 120 dpi.

The distribution and intensity of *B. melitensis* DNA signals in the examined sections were determined by ISH staining and are summarized in Tables 1A and 1B. Hybridization signals of *B. melitensis* were widely distributed in the heart, liver, spleen, lungs, kidneys, lymph nodes, testes, duodenum, jejunum, ileum, abomasum, and bladder.

The strongest hybridization signals were detected at 7 and 15 dpi, after which the signals gradually cleared, and no signal was detected from any of the organs or tissues after 120 dpi. Infected cells were mainly found among macrophages, reticuloendothelial cells, neutrophils, and epithelial cells.

In the hearts, moderate signals were detected in the macrophages and neutrophils from 7 to 60 dpi. In the liver, positive signals were localized in hepatic parenchymal cells and macrophages from 7 to 30 dpi.

In the spleens, the majority of the signals were detected in the germinal center of white pulp, the marginal zone, periarteriolar lymphatic sheath, spleen trabecula, and splenic sinus. Stronger signals appeared in the macrophages at 7 dpi (Figure 3A) and gradually decreased and localized to red pulp and white pulp after 15 dpi.

In the lungs, the signals could only be detected at 15 and 30 dpi. The majority of the signals were detected in the alveolar epithelial cells, bronchial epithelial cells, macrophages, and neutrophil infiltration between alveoli (Figure 3B).

In the kidneys, the signals were detected from 7 to 90 dpi; the strongest signal was found at 15 dpi and it persisted until 90 dpi. The majority of the signals were detected in the epithelial cells of glomeruli, collecting ducts, and proximal and distal convoluted tubule (Figure 3C).

In the lymph nodes, the signals were mainly located in the macrophages, neutrophils, and reticuloendothelial cells (Figure 3D) of the germinal centers, loose connective tissue around the lymphoid follicle, medullary cords, and sinuses. Infected cells were detected in all of the lymph nodes at the initial stage of infection, but the submandibular lymph nodes contained the only tissue detected at 120 dpi. The strongest signal was found at 7 dpi, and it decreased gradually. More prominent signals were detected in the prescapular and parotid lymph nodes as compared to the other lymph nodes, which might be associated with the inoculation site of *B. melitensis* 16M.

**Table 1A.** The distribution of detectable *Brucella* nucleic acid in the formaldehyde-fixed paraffin-embedded tissues detected by ISH staining.

DPI	Sheep no.	Heart	Liver	Spleen	Lung	Kidney	Testis	Duodenum	Jejunum	Ileum	Abomasum	Bladder
7	1	++	+++	+++	-	++	-	++	++	+	+	+
	2	++	+++	+++	-	++	-	+++	++	+	+	+
15	3	++	+++	++	+++	+++	++	+	+	+	+	+
	4	++	++	++	+++	+++	+	-	-	+	+	+
30	5	+	+	++	+	+	-	-	+	+	-	-
	6	+	+	++	+	++	-	-	+	-	+	-
60	7	-	-	+	-	+	-	+	-	-	-	-
	8	+	-	+	-	+	-	+	-	-	-	-
90	9	-	-	-	-	-	-	-	-	-	-	-
	10	-	-	-	-	+	-	-	-	-	-	-
120	11	-	-	-	-	-	-	-	-	-	-	-
	12	-	-	-	-	-	-	-	-	-	-	-
180	13	-	-	-	-	-	-	-	-	-	-	-
	14	-	-	-	-	-	-	-	-	-	-	-

-: Negative; +: limited positive staining, less than 1 cell per high power field; ++: moderate positive staining, approximately 1 cell per high power field; +++: extensive positive staining, more than 1 cell per high power field; ISH: in situ hybridization.

**Table 1B.** The distribution of detectable *Brucella* nucleic acid in the formaldehyde-fixed paraffin-embedded tissues detected by ISH staining (continued).

DPI	Sheep no.	Prescapular LN	Submaxillary LN	Parotid LN	Inguinal LN	Iliac LN	Portal LN	Pulmonary LN	Reniportal LN	Mesenteric LN
7	1	+++	+++	+++	++	+++	+++	++	++	++
	2	+++	++	+++	++	+++	+++	+++	++	++
15	3	+++	++	++	++	++	++	++	+	+++
	4	+++	+++	+++	++	+	+++	+++	+	++
30	5	++	++	++	+	++	+	+++	++	++
	6	+++	+++	++	+++	++	+	+	+	++
60	7	++	+	+	+	-	-	-	-	+
	8	++	+	+++	+	+++	-	-	-	+++
90	9	++	-	-	-	-	-	-	-	-
	10	-	+	+	++	-	-	-	-	-
120	11	-	-	-	-	-	-	-	-	-
	12	-	+	-	-	-	-	-	-	-
180	13	-	-	-	-	-	-	-	-	-
	14	-	-	-	-	-	-	-	-	-

-: Negative; +: limited positive staining, less than 1 cell per high power field; ++: moderate positive staining, approximately 1 cell per high power field; +++: extensive positive staining, more than 1 cell per high power field; ISH: in situ hybridization; LN: lymph node.

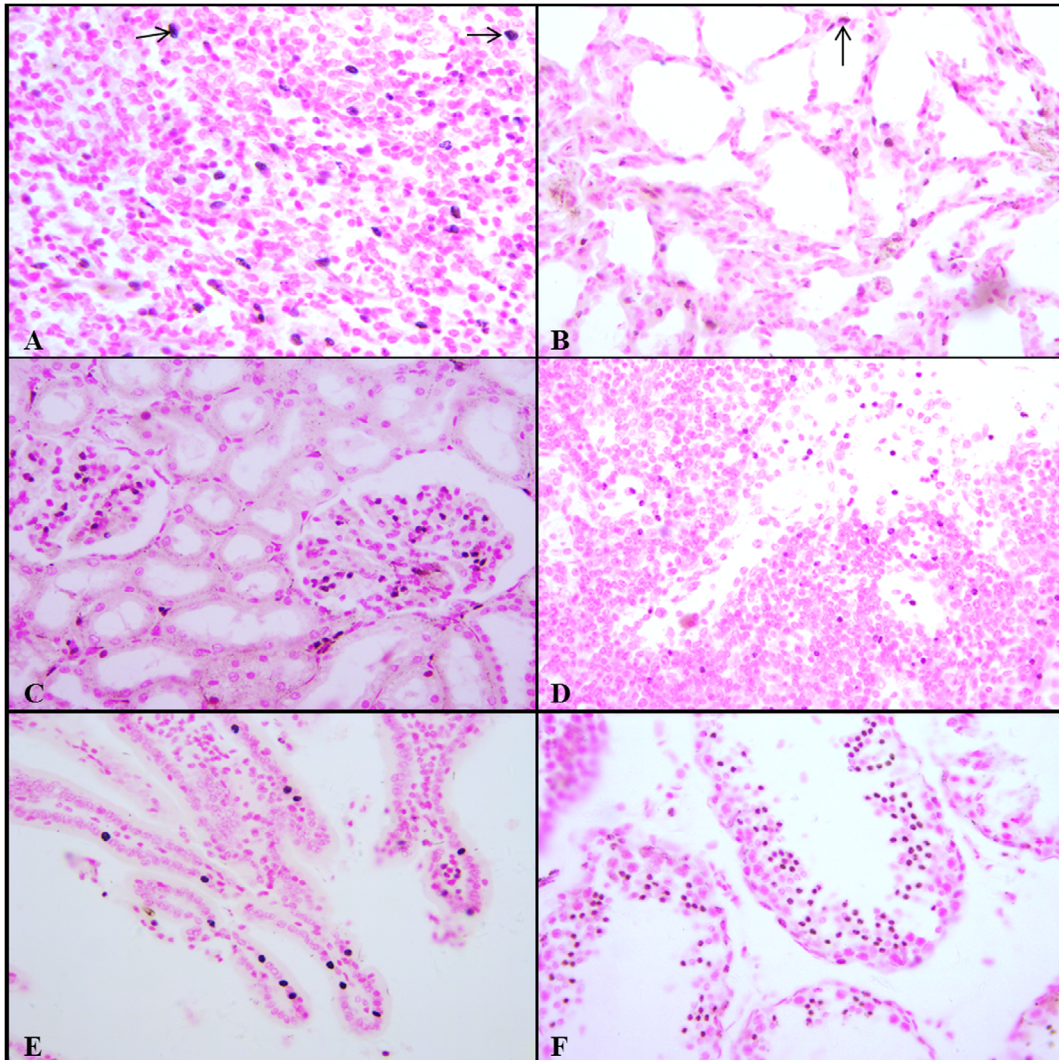


**Figure 3.** (A) Spleen, 60 dpi. *B. melitensis* DNA localized in macrophages (arrow) of white pulp. In situ hybridization, nuclear fast red counterstain. (B) Lung, 15 dpi. *B. melitensis* DNA localized in the macrophages (arrow), alveolar epithelial cells and inflammatory cells infiltrated. In situ hybridization, nuclear fast red counterstain. (C) Kidney, 30 dpi. *B. melitensis* DNA localized in epithelium of renal tubule and collecting duct. In situ hybridization, nuclear fast red counterstain. (D) Inguinal lymph node, 30 dpi. *B. melitensis* DNA localized in the macrophages, neutrophils, and reticuloendothelial cells of medullary sinus. In situ hybridization, nuclear fast red counterstain. (E) Duodenum, 30 dpi. *B. melitensis* DNA localized in epithelial cells of intestinal mucosa and intestinal gland. In situ hybridization, nuclear fast red counterstain. (F) Testicle, 90 dpi. *B. melitensis* DNA localized in epithelial cells of seminiferous tubules. In situ hybridization, nuclear fast red counterstain.

Among the small intestines, the intensity and amount of hybridization signals were the highest in the duodenum, second highest in the jejunum, and the lowest in the ileum. The strongest signal was found at 7 dpi, and it decreased gradually. In the duodenum, the majority of the signals were detected in the epithelial cells of intestinal mucosa and the intestinal gland (Figure 3E). In the jejunum, the signals were detected in intestinal epithelial cells. In the ileum, the signals were detected in the epithelial cells of the mucosa and lamina propria, the macrophages and lymphoid cells of the lamina propria, and the intestinal gland.

Some hybridization signals were detected in the bladder, abomasum, and testes. In the bladder, the signal was mainly found at 7 and 15 dpi. In the abomasum, the positive signal was chiefly localized to the epithelial cells at 7 and 15 dpi. In the testes, the signal was localized to the epithelial cells of seminiferous tubules at 7 dpi (Figure 3F). However, no positive signal was detected in skeletal elements or smooth muscle, or in the epididymis (rams), mammary glands, or uterine horn (nonpregnant ewes).

#### 4. Discussion

It is well known that *Brucella* has persisted for long periods in some infected individuals, with the specific antibodies also persisting for a long time, even lifelong. These seropositive reactors were traditionally culled in animal brucellosis eradication campaigns. However, based on an animal's genetic background, age, immunological status, and sexual maturity and the *Brucella* inoculation route, dose, and virulence, some infected animals can recover from infection with a low dose of *Brucella*, and some animals even resist infection by *Brucella* spp. Usually, animals infected by *Brucella* spp. show complicated manifestations; some individuals of the same species show discrepancies in resistance against *Brucella* infection. Some animals were indicated *Brucella*-free in bacterial culture with transient seropositive responses, while others might include a small number of *Brucella* with seronegative responses. This suggests that the persistence of *Brucella* in infected animals is not necessarily associated with antibodies. In this study, correlations between the bacterial loads and antibody titers in infected sheep were explored by examining *Brucella* loads in the different samples and the agglutinating antibodies at different times following infection. These results were similar to those found in previous studies with experimental goats (13,15). In our bacteriological examination, *Brucella* in tissue samples was highly detectable at 7 dpi, with peak loads at 15 dpi, followed by a gradual reduction from 15 to 120 dpi. From 120 to 360 dpi *B. melitensis* in the tissue samples was always undetectable. Meanwhile, the seroagglutinating antibody in infected sheep was detectable at 7 dpi, reached a peak titer at 15 dpi, and then gradually reduced from 15 to 240 dpi. At 270 dpi, the serum samples collected from the infected animals still presented agglutination but were negative based on the antibody titers, and at 360 dpi the agglutination phenomenon disappeared in the samples. This study indicated that there might be a positive correlation between the bacterial loads and agglutinating antibody titers in the experimental sheep, which was generally consistent with observations in infected young goats (13,16). Our results also showed that the greater the *Brucella* bacterial loads were in vivo, the higher the agglutination antibody titers were in the experimental sheep. When the seroagglutinating antibody titers were reduced to below 1:400, the *Brucella* strain was difficult to isolate from the samples of infected animals in our experiments. It was suggested that the higher agglutination titers might be associated with the activity of the live *B. melitensis* strain in infected animals.

*Brucella* spp. had a strong tropism to the uterus during the last trimester of gestation, causing chronic infection

of the mammary glands throughout the lifetime (17). Therefore, the mammary gland was thought to be a target organ, by which *Brucella* was transmitted from the infected animal to human through the contaminated milk (18). In this work, live *Brucella* was not detected in the mammary glands and uteri of the nonpregnant ewes throughout our experiment, indicating that these organs might not be easily infected during nonpregnancy.

Clinically, *Brucella* spp. infected individuals might be bacteria carriers and show strong serum agglutination responses, but some individuals have no serum antibodies. For bacteria carriers without seroreactivity, no exact detection method was available in animal brucellosis eradication campaigns, and so detection methods for infected animals that carried *Brucella* without seropositivity responses should be enhanced in future research. Moreover, this study also showed that most of the samples were positive for *Brucella* detection at the initial stage, but almost all the samples examined were negative at 180 dpi, suggesting that *B. melitensis* might have been gradually eliminated by the host immunity or that the number of bacteria might have become too low to be detected in vivo. For the bacteriological examination, ISH could be complementary to bacterial isolation for pathogen detection, and there was consistency between bacteriological examination and the ISH method. For example, *Brucella* in tissue samples in this study was highly detectable at 7 dpi, with the highest detection rate at 15 dpi, followed by a gradual reduction from 15 to 120 dpi by the two methods. From the bladder, duodenum, jejunum, ileum, and abomasum, no live bacteria were isolated, but the specific DNA signals were positive, which indicated that ISH might be a good choice for *Brucella* detection in consideration of the biological safety in operation (12).

In conclusion, the present study indicated that syngenetic succession of *Brucella* loads was accompanied with that of anti-*Brucella* agglutinating antibody responses in experimentally infected rams and nonpregnant ewes. We observed *Brucella melitensis* survival in in vivo predilection sites and a positive correlation between bacterial loads and agglutination antibody titers in the experimental sheep; the more bacteria that survived in the body, the higher the agglutination antibody titers were in the sera. The detection of the agglutinating antibody titers might provide insight into a low-cost method of reducing false-culling of the resistant animals as much as possible in combating against animal brucellosis.

#### Acknowledgments

This work was supported by the National Natural Science Foundation of China (Project no. 31372446) and the National Basic Research Program of China (973 Program, 2010CB530202).

## References

1. Enright FM. The pathogenesis and pathobiology of *Brucella* infection in domestic animals. In: Mielsen K, Duncan JR, editors. Animal Brucellosis. Boca Raton, FL, USA: CRC Press; 1990. pp. 301–320.
2. Chand P, Sadana JR, Malhotra AK. Epididymo-orchitis caused by *Brucella melitensis* in breeding rams in India. Vet Rec 2002; 150: 84–85.
3. Payne JM. The pathogenesis of experimental brucellosis in virgin heifers with and without continuous progesterone treatment. J Endocrinol 1960; 20: 345–354.
4. Suraud V, Jacques I, Olivier M, Guilloteau LA. Acute infection by conjunctival route with *Brucella melitensis* induces IgG+ cells and IFN-gamma producing cells in peripheral and mucosal lymph nodes in sheep. Microbes Infect 2008; 10: 1370–1378.
5. Durán-Ferrer M, León L, Nielsen K, Caporale V, Mendoza J, Osuna A, Perales A, Smith P, De-Frutos C, Gómez-Martín B et al. Antibody response and antigen-specific gamma interferon profiles of vaccinated and unvaccinated pregnant sheep experimentally infected with *Brucella melitensis*. Vet Microbiol 2004; 100: 219–231.
6. Mense MG, Van De Verg LL, Bhattacharjee AK, Garrett JL, Hart JA, Lindler LE, Hadfield TL, Hoover DL. Bacteriologic and histologic features in mice after intranasal inoculation of *Brucella melitensis*. Am J Vet Res 2001; 62: 398–405.
7. Hamdy ME, Amin AS. Detection of *Brucella* species in the milk of infected cattle, sheep, goats and camels by PCR. Vet J 2002; 163: 299–305.
8. Ramin B, Macpherson P. Human brucellosis. BMJ 2010; 341: c4545.
9. Adams LG. The pathology of brucellosis reflects the outcome of the battle between the host genome and the *Brucella* genome. Vet Microbiol 2002; 90: 553–561.
10. Alton GG, Jones LM, Pietz DE. Laboratory Techniques in Brucellosis. Geneva, Switzerland: World Health Organization; 1975.
11. Elfaki MG, Al-Hokail AA, Nakeeb SM, Al-Rabiah FA. Evaluation of culture, tube agglutination, and PCR methods for the diagnosis of brucellosis in humans. Med Sci Monit 2005; 11: MT69–MT74.
12. Wellinghausen N, Nöckler K, Sigge A, Bartel M, Essig A, Poppert S. Rapid detection of *Brucella* spp. in blood cultures by fluorescence in situ hybridization. J Clin Microbiol 2006; 44: 1828–1830.
13. Cheville NF, Olsen SC, Jensen AE, Stevens MG, Florance AM, Houng HS, Drazek ES, Warren RL, Hadfield TL, Hoover DL. Bacterial persistence and immunity in goats vaccinated with a purE deletion mutant or the parental 16M strain of *Brucella melitensis*. Infect Immun 1996; 64: 2431–2439.
14. Bricker BJ, Halling SM. Differentiation of *Brucella abortus* bv. 1, 2, and 4, *Brucella melitensis*, *Brucella ovis*, and *Brucella suis* bv. 1 by PCR. J Clin Microbiol 1994; 32: 2660–2666.
15. Muñoz PM, de Miguel MJ, Grilló MJ, Marín CM, Barberán M, Blasco JM. Immunopathological responses and kinetics of *Brucella melitensis* Rev 1 infection after subcutaneous or conjunctival vaccination in rams. Vaccine 2008; 26: 2562–2569.
16. Elzer PH, Hagius SD, Davis DS, DelVecchio VG, Enright FM. Characterization of the caprine model for ruminant brucellosis. Vet Microbiol 2002; 90: 425–431.
17. Bellaire BH, Elzer PH, Baldwin CL, Roop RM. Production of the siderophore 2,3-dihydroxybenzoic acid is required for wild-type growth of *Brucella abortus* in the presence of erythritol under low-iron conditions in vitro. Infect Immun 2003; 71: 2927–2832.
18. Ko J, Splitter GA. Molecular host-pathogen interaction in brucellosis: current understanding and future approaches to vaccine development for mice and humans. Clin Microbiol Rev 2003; 16: 65–78.